Scheduling of Mobile Charging Stations with Local Renewable Energy Sources

Abdullah Kürşat Aktar[1], Akın Taşcıkaraoğlu[1,*], João P. S. Catalão[2]

[1]*Electrical and Electronics Engineering Department, Mugla Sitki Kocman University, Mugla, Turkey*

[2] *Research Center for Systems and Technologies (SYSTEC), Advanced Production and Intelligent Systems Associate Laboratory (ARISE), Faculty of Engineering, University of Porto, 4200-465 Porto, Portugal*

** akintascikaraoglu@mu.edu.tr*

Abstract

Due to the depletion of fossil resources and increasing environmental concerns, electric vehicles (EVs) have been attracting more attention at the last decade. Their extensive integration into the energy systems, however, has led to numerous operational and technological challenges, especially during their bulk charging. In this study, an optimization algorithm based on mixed integer linear programming is proposed to dispatch mobile charging stations (MCSs), which have emerged as both an alternative and supplement to permanent charging stations (PCSs). It is aimed to mitigate the number of EVs that cannot be charged in PCSs, due mostly to the limited charging unit capacity and prolonged waiting times, by using an MCS. Five determinative cases involving a combination of different operating and pricing mechanisms are evaluated. The results reveal that the use of the MCS provides both economic and operational benefits. In the best case determined according to the result of the comparisons with various pricing mechanisms, the MCS provides an operational improvement of 64.3% compared to the case without the MCS. The quantity of EVs requesting service is 1074 in all cases, while 986 EVs are served in the case with the best results. Besides, a profit increase of 46% is achieved for the cases in which dynamic pricing is applied. An important point to note is that with the incentive mechanism applied, there is a significant increase in the profit in Case 5, while the number of EVs served is 967. In case 4, without incentive mechanism, the number of EVs served is 968.

Keywords: Electric vehicle, energy storage, mobile charging station, renewable energy, vehicle-to-vehicle charging.

Nomenclature

The abbreviations, sets, parameters and variables used in this paper are listed below.

A. Abbreviations

ESS	Energy storage system.
EV	Electric vehicle.
MCS	Mobile charging stations.
MV	Missing vehicle.
PCS	Permanent charging station.
RES	Renewable energy source.
SOE	State-of-energy.
$V2V$	Vehicle-to-vehicle.

B. Sets

B_l^{ij}	Index of sending end i buses and receiving end j buses.
i	Index of buses.
l	Index of lines.
t	Index of time interval for energy flow.
tt	Index of time interval for travel of MCS.
v	Index of MCS velocity.

C. Parameters

A	MCS Vehicle frontal area [m^2].
B_l	Susceptance of line l [pu].
C_d	Aerodynamic drag coefficient.
C_{rr}	Coefficient of rolling resistance.
CE^{MCS}	Charging efficiency of the MCS battery [%].
CS^{MCS}	Number of charging and discharging socket of MCS.
CS^{PCS}	Number of charging and discharging socket of PCS.
DE^{MCS}	Discharging efficiency of the MCS battery [%].
EC^{MCS}	Energy consumption of MCS [kWh].
$F_{v,tt}^{a}$	Aerodynamic drag force of EV in time interval tt [kg.m/s^2].
$F_{v,tt}^{ac}$	Acceleration force of EV in time interval tt [kg.m/s^2].
F_{tt}^{g}	Gravity force of EV in time interval tt [kg.m/s^2].
F_{tt}^{r}	Rolling friction force of EV in time interval tt [kg.m/s^2].
$F_{v,tt}^{t}$	Total traction force of EV in time interval tt [kg.m/s^2].
f_m	Mass factor.
g	Gravity of earth [m/s^2].
M^{MCS}	Mass of MCS [kg].
$M_{i,l}^{F}$	Coefficient is 1 if line l of bus i is receiving end; -1 if line l of bus i is sending end; 0 if it is not both.
$M_{i,l}^{L}$	Coefficient is 1 if line l of bus i is sending end; 0 if it is not.
$M_{l,i}^{W}$	Coefficient that belongs to bus i and line l is obtained from transpose of $M_{i,l}^{F}$ matrix.

$P_{v,tt}^{ve}$ Electrical power demand of MCS in time interval tt [W].
$P_{v,tt}^{vm}$ Mechanical power demand of MCS in time interval tt [W].
$P_{i,t}^{L,total}$ Active power demand of bus i in time interval t [pu].
$Price_{i,t}$ Electricity price of bus i in time interval t [€/kWh].
$P_{i,t}^{CPD}$ Charging power demand of bus i in time interval t [pu].
$P_{i,t}^{W}$ Active power generation by wind farm at bus i in time interval t [pu].
$P_{i,t}^{BM}$ Active power generation by biomass power plant at bus i in time interval t [pu].
$Q_{i,t}^{L}$ Reactive power demand of bus i in time interval t [pu].
$R_i^{MCS,\mathrm{ch}}$ Charging rate limit of MCS that is connected to bus i [kW].
R_i^{MCSdis} Discharging rate limit of MCS that is connected to bus i [kW].
$R_i^{PCS,PD}$ Discharging rate limit of PCS that is connected to bus i [kW].
R_l Resistance of line l [pu].
$SOE^{MCS,ini}$ Initial SOE of the MCS [kWh].
$SOE^{MCS,max}$ Maximum SOE of the MCS [kWh].
$SOE^{MCS,min}$ Minimum SOE of the MCS [kWh].
V_{max} Permitted maximum voltage level of buses [pu].
V_{min} Permitted minimum voltage level of buses [pu].
$V_{v,tt}^{MCS}$ MCS vehicle speed [m/s].
$V_{v,tt}^{W}$ Wind speed [m/s].
X_l Reactance of line l [pu].
α Acceleration [m^2/s].
η_d Driving efficiency.
ρ Air density [kg/m^3].
θ Road slope angle [°].
ΔT Time period [min].

D. Variables

$m1_{i,t}$ Binary variable (1 if the MCS is connected to bus i in time interval t; 0 otherwise).
$m2_t$ Binary variable (1 if the MCS is on travel in time interval t; 0 otherwise).
$m3_{j,t}$ Binary variable (1 if the MCS leaves the bus j during time interval t; 0 otherwise).
$m4_{i,t}$ Binary variable (1 if the MCS is connected to the bus i during time interval t; 0 otherwise).
$P_{i,t}^{G}$ Total active power of bus i in time interval t [pu].
$P_{i,t}^{L}$ Total power demand of bus i in time interval t [pu].
$P_{i,t}^{S}$ Total power flowing from transformer to bus i in time interval t [pu].
$P_{i,t}^{MCS,ch}$ Charging power by MCS that is connected to bus i in time interval t [kWh].
$P_{i,t}^{MCS,dis}$ Discharging power by MCS that serves next to PCS bus i in time interval t [kWh].
$P_{i,t}^{PCS,PD}$ Charging power by PCS to charge EVs in the queue at bus i in time interval t [kWh].
$P_{l,t}^{\mathrm{loss}}$ Total active power loss of line l in time interval t [pu].
$\hat{P}_{l,t}^{\mathrm{loss}}$ Model variable to represent total active power loss of line l in time interval t [pu].
$P_{l,t}^{r}$ Total active power of line l in time interval t [pu].
$Q_{l,t}^{\mathrm{loss}}$ Total reactive power loss of line l in time interval t [pu].

$Q_{i,t}^{G}$	Total reactive power of bus i in time interval t [pu].
$Q_{l,t}^{r}$	Total reactive power of line l in time interval t [pu].
SOE_{t}^{MCS}	SOE of the MCS battery in time interval t [kWh].
$u_{i,t}^{ch}$	Binary variable (1 if the MCS is charging in time interval t; 0 otherwise).
$u_{i,t}^{dch}$	Binary variable (1 if the MCS is discharging in time interval t; 0 otherwise).
$V_{i,t}$	Voltage magnitude of bus i in time interval t [pu].
$W_{i,t}$	Equivalent of cosine term of power flow equation on line (i,j) in time interval t [pu].
$W_{r,t}$	Square of voltage magnitude at receiving end bus r $(r \in i)$ in time interval t [pu].

1. Introduction

1.1 Literature Overview

Due to the recent political problems affecting many countries in the world, inter-country conflicts such as the Russia-Ukraine war and the lasting effects of the pandemic, the efforts have been making to create a stable chain in energy supply especially. The improvement in the world energy sector can be expressed with an increase of 4%, which also includes approximately 1000 TWh electrical energy demand in 2021 [1]. The fact that the daily energy demand of the European Union was 120 GW in 2020 and is foreseen to reach 270 GW by 2050 shows that the importance of energy security will gradually increase [1]. Besides, 90% of the energy generation increase between 2020 and 2050 in non-OECD countries where the economic growth is faster is expected to come from renewable energy sources (RESs) [2]. This projection is particularly important in ensuring the national energy security of the countries concerned.

Residential electrical energy demand is estimated to increase at least 20% by 2050 according to the report from the U.S. Department of Energy [3]. With the increase in the number of electric vehicles (EVs) in the near future, the charging demand power will take its place in the residential energy demand. Considering that the total number of 120,000 EVs sold in 2012 was reached in only one week in 2021, it is clear that the sales would gain momentum and reach large quantities [4]. In order to maintain the sustainability and security of the existing electricity systems, it is important to ensure more effective use of the systems and encourage the new investments.

Inadequate charging infrastructure, the effect of charging power demand on grids, the cost of purchasing EVs and the efficiency of their battery especially in different weather conditions can be cited as the important obstacles to the more widespread of EVs [5]. The problem of climate change, political situations in the world and recent developments in technology, however, encourage the countries to pay more attention to these obstacles. For example, in the research conducted in [6], it is mentioned that the government is eager to transform the transportation sector of India, where air pollution is very high, to 100% EVs. In another study [7], it is stated that the Hainan Free Trade Port Scheme aims to minimize the carbon emissions in Hainan by 2030 by mandating the use of new generation EVs.

While the number of EVs in the transportation sector has been increased, different forms of charging structures have been emerging. There are on-board and off-board, residential and commercial, AC and DC variants created according to the different standards such as SAE and IEC [8]. Residential chargers operate in AC mode and take a longer period to reach the full charge at low power, while the charging times of three-phase commercial versions are much less. As an alternative, DC charging stations offer a higher power and thereby a higher range for EVs in a short time. In an electrical grid with all the charging options, the control of the charging load demand is crucial for the reliable and effective operation of the grid. In the study conducted in [9], it is stated that the impact on the grid can be reduced if the EVs are charged in a coordinated manner during off-peak hours. In addition, the coordinated charging of EVs is targeted in [10] to achieve a load curve where the peak-to-valley difference is minimized, and it is proved that generation cost and pollutant emission can be reduced in the designed microgrid system. In another study [11], the residential load and EV charging energy demand are supplied by considering a smart home system with RES while keeping the comfort level of the user at a certain value. While it is considered positive that the created algorithm reduces the average energy costs by 20%, the usage of commercial or public charging stations may also provide cheaper charging service under conditions of the flexible charging hours and time intervals. In a study in which a public charging station is used for faster charging, when EV users determine their priorities such as the amount of energy to be consumed, a guidance is made to reduce the waiting time for charging and the impact of EV on the grid [12]. Moreover, the RESs and charging stations are considered together in order to balance the fluctuating energy production of RESs and the varying load demand of EV users, and to accomplish a cost-effective system [13]. In addition, it is stated in [14] that when a similar approach is applied in ultra-fast charging stations with an energy storage system (ESS), it produces remarkable results on the operating profitability.

Aggregators, who can create a fleet by making special agreements with EV owners and use this fleet for profitable energy trade, have emerged as a stakeholder of the newly formed electrical system. In [15], while making a profit by using charging and discharging operations, the aggregator provides technical support to the grid operator in terms of losses and bus voltage. In another study [16], the EV owners charge their EVs with low energy costs in a microgrid with RESs and the profit increases by about 17% while the local load demand is met. Besides, in [17], it is stated that the coordinated use of EVs in the bidirectional energy flow reduces the dependence on conventional energy sources by approximately 29%, resulted in a more profitable microgrid operation. In another study that supports the same idea [18], an energy credit mechanism is established to enable the end-user to access more affordable energy at peak load time in a system with an EV fleet and PV systems. In [19], it is concluded that the large-capacity mobile ESS constituted from an EV fleet operates at different bus nodes and provides both load curve flattening capability and economic contribution to the stakeholders.

While the use of EVs has been accelerated by the technical, legal and social contribution of all stakeholders, it is necessary to take new preventions to ensure the sustainability and reliability of the energy systems. Apart from the different mechanisms

mentioned above, mobile charging stations (MCSs) can be also shown as a new player of the system. MCSs might remove one of the barriers to EV use by offering a fast and economical solution in areas where the electricity grid infrastructure is insufficient. The rapid installation of MCSs next to permanent charging stations (PCSs) and their use in the bus nodes according to the load demand can be expressed as their most important advantages [20]. In addition, when used with different system components such as combined heat power unit and ESS, they can make a remarkable economic contribution to the commercial enterprises [21]. The fact that the installation of a charging station infrastructure especially in rural areas is an expensive solution [22] and that a truck with a battery capacity of 2.1 MWh can charge 10 EVs simultaneously at their rated power [23] reveal the feasibility and applicability of MCSs.

In the study conducted in [24], the MCS is dynamically dispatched to serve EVs, resulting in a reduction in charging expenditures and an increase in the number of EVs served. Besides, for the charging operation of the MCS, the load status of the electricity grid and the energy consumption of the MCS are considered to enable the system to produce more realistic results. In another research [25], which prioritizes reducing the number of waiting EVs in the queue, the surplus renewable energy generation is stored in the battery of the MCS and used for the EV charging. In addition, including the energy consumption equations of a self-electric powered MCS and creating different bus node energy price tariff especially for RESs connected to buses in the mentioned study provide more effective and economical management of the system. An MCS is directed to shorten the waiting and charging time by taking into account the congestion of the PCS and the electrical grid usage rate in [26] by an algorithm that makes the charging plan for the EVs. It is indicated that the operating cost of the MCS and the management of the electrical grid to perform valley filling and peak shaving operations can be considered to increase the performance of the algorithm.

In this study, unlike the studies mentioned above, an MCS is directed to the most appropriate bus node to provide the charging service to EVs by considering the load demand of the grid and number of EVs waiting for charging. In addition, the travel time of the MCSs between different bus nodes and their energy consumption are taken into account while determining the bus node to be served by the MCS. Moreover, the EVs with different battery capacities are considered in the proposed system and different cases including the one where the MCS is charged with the energy from renewable power plants are examined.

1.2 Content and Contributions

This study considers a distribution system with various consumer types, mid-sized wind and biomass energy power plants, PCSs and an MCS that can deliver bidirectional energy flow. The MCS is an EV that travels with its own power and has charging terminals on it. In order to meet the demand for the EV loads during the peak energy period, it is proposed that the MCS can act as a mobile ESS. Besides, the MCS battery is charged during periods of low energy demand and low prices, targeting both operational and economic benefits at peak time. While the MCS can be charged at multiple points of the considered distribution system, it can only be used for discharging at a fewer point. The routing constraints, such as the time interval between the buses that the MCSs need to

travel, are taken into consideration while determining these locations. Only a travel route between any two bus nodes is considered and in order not to distract from the main objectives of the study, the daily and seasonal changes in traffic conditions are not considered.

The aim of the study is to serve the highest number of EVs by directing the MCS according to the number of EVs coming to the PCSs to receive the charging service. To this end, an algorithm taking the load demand of the grid into account and carrying out effective grid management by maintaining peak shaving and valley filling operations is developed. Besides, an economic benefit is achieved by taking advantage of the dynamic energy prices in determining the charging-discharging periods of the MCS.

The contribution of this study is multifaceted:

- The proposed energy management algorithm investigates the function of MCSs in improving grid operation and minimizing the number of EVs waiting for charging.
- The economic operation of the MCS, which has the option of using the energy from the RESs at a lower cost, and the energy transfer operations through vehicle-to-vehicle (V2V) technology are evaluated in the proposed system.
- During the high charging demand periods, the operation of MCS to mitigate the stress on the electrical grid by supplying some portion of the energy to EVs is analyzed.

1.3 Organization of the Paper

The rest of the paper is organized as follows. In Section 2, the architecture of the system considered is presented, which includes the power exchange equations of electrical grid and energy consumption, and mobility equations of MCS. Then, the efficiency of the proposed optimization algorithm is evaluated with five case studies in Section 3. Finally, the study is concluded in Section 4.

2. Methodology

In the proposed framework, a distribution system of 15 buses with varying load characteristics is implicated, as shown in Fig. 1. In order to provide charging service to EVs, two PCSs are connected to different bus nodes and powered by the low voltage (LV) side of the transformer. An MCS with charging sockets and a battery can charge at the predefined bus nodes and make V2V operations without connecting to the grid at the PCS points. It is assumed that the PCSs and MCS belong to the distribution system operator and are used to balance the load demand of the grid, coordinate the charging of EVs, and enhance the economic benefits. The main energy provider of the system is the transformer connected to the Bus 1, and in different bus nodes, a biomass power plant and a wind farm generate energy to meet some portion of the energy demand. The designed system aims to provide the optimum charging service to EVs by MCS and PCSs, taking the load demand of the grid and energy prices into account. The optimization problem with the related constraints and mathematical expressions are given by (1) – (31).

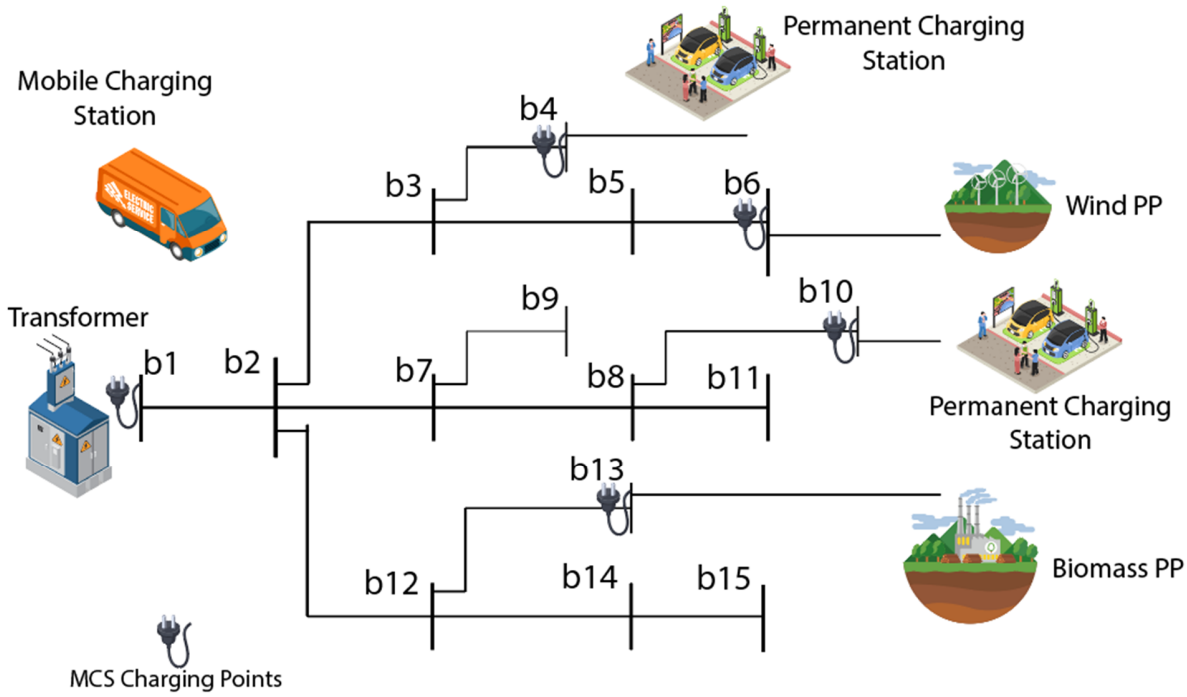

Fig. 1. Block diagram of the distribution system considered.

$$Minimize\ MV = \sum_{t}\sum_{i}((P_{i,t}^{CPD} - P_{i,t}^{MCS,dis} - P_{i,t}^{PCS,PD}) \cdot \Delta T) \tag{1}$$

subject to:

$$P_{i,t}^{G} - P_{i,t}^{L} = \sum_{l \in B_l^{ij}} \left(M_{i,l}^{F} \cdot P_{l,t}^{r} + M_{i,l}^{L} \cdot P_{l,t}^{\text{loss}}\right) \ \forall i,t \tag{2}$$

$$Q_{i,t}^{G} - Q_{i,t}^{L} = \sum_{l \in B_l^{ij}} \left(M_{i,l}^{F} \cdot Q_{l,t}^{r} + M_{i,l}^{L} \cdot Q_{l,t}^{\text{loss}} - B_l \cdot M_{l,i}^{W} \cdot W_{i,t}\right) \ \forall i,t \tag{3}$$

$$P_{i,t}^{G} = P_{i,t}^{S} + P_{i,t}^{W} + P_{i,t}^{BM} \ \forall i,t \tag{4}$$

$$P_{i,t}^{L} = P_{i,t}^{L,total} + P_{i,t}^{MCS,\text{ch}} + P_{i,t}^{PCS,PD} \ \forall i,t \tag{5}$$

$$W_{i,t} = V_{i,t}^{2} \ \forall i,t \tag{6}$$

$$P_{l,t}^{\text{loss}} = 2 \cdot R_l \cdot \hat{P}_{l,t}^{\text{loss}} \ \forall l,t \tag{7}$$

$$X_l \cdot P_{l,t}^{\text{loss}} - R_l \cdot Q_{l,t}^{\text{loss}} = 0 \ \forall l,t \tag{8}$$

$$\sum_{i}\left(M_{l,i}^{W} \cdot W_{i,t}\right) - 2 \cdot \left(R_l \cdot P_{l,t}^{r} + X_l \cdot Q_{l,t}^{r}\right) = R_l \cdot P_{l,t}^{\text{loss}} + X_l \cdot Q_{l,t}^{\text{loss}} \ \forall l,t \tag{9}$$

$$2 \cdot \hat{P}_{l,t}^{loss} \cdot W_{r,t} \geq {P_{l,t}^{r}}^{2} + {Q_{l,t}^{r}}^{2} \ \forall l,t \tag{10}$$

$$V_{min}^{2} \leq W_{i,t} \leq V_{max}^{2} \ \forall i,t \tag{11}$$

$$0 \leq P_{i,t}^{MCS,\text{ch}} \leq R_i^{MCS,\text{ch}} \cdot u_{i,t}^{ch} \ \forall i,t \tag{12}$$

$$0 \leq P_{i,t}^{MCS,dis} \leq R_i^{MCS,dis} \cdot u_{i,t}^{dch} \ \forall i,t \tag{13}$$

$$u_{i,t}^{ch} + u_{i,t}^{dch} = m1_{i,t} \tag{14}$$

$$0 \le P_{i,t}^{PCS,PD} \le R_i^{PCS,PD} \; \forall i,t \tag{15}$$

$$\mathrm{SOE_t^{MCS}} = \mathrm{SOE_{(t-1)}^{MCS}} + \sum_i \left(\mathrm{CE^{MCS}} \cdot \mathrm{P_{i,t}^{MCS,ch}} - \frac{\mathrm{P_{i,t}^{MCS,dis}}}{\mathrm{DE^{MCS}}} \right) \cdot \Delta \mathrm{T} - (\mathrm{EC^{MCS}} \cdot m2_t) \; \forall \mathrm{t} \tag{16}$$

$$SOE^{MCS,min} \le SOE_t^{MCS} \le SOE^{MCS,max} \; \forall t \tag{17}$$

$$SOE_t^{MCS} = SOE^{MCS,ini} \; if \; t = 1 \tag{18}$$

As mentioned above, the main objective of the proposed optimization problem based on mixed integer linear programming is to minimize the difference between the total hourly power demand of EVs and the power supplied by PCS and MCS, as given in (1). The number of EVs that cannot be charged is calculated by subtracting the number of EVs arriving for charging and the sum of the active sockets of the PCS and MCS in each time interval. The active and reactive power equations of the electrical network are given by (2) and (3), respectively. The wind farm, biomass power plant and transformer are on the side that supplies energy to the system as shown by (4). Domestic and commercial loads connected to each bus node and EVs coming to the PCS points constitute the consumer side of the system as shown by (5). Moreover, the MCS acts as a consumer while charging its battery, and as a producer when charging EVs due to its support to the grid. The AC power flow equations from [27] are presented in (6)-(11). The linearization of the aforementioned equations is explained in detail in [27]. By selecting the proper solver such as MOSEK, these equations expressed in a second-order cone formulation may be utilized in a linear optimization method.

Power limits of the MCS's charging and discharging operations are given in (12) and (13), respectively. Thanks to the binary variables in (14), simultaneous charging and discharging of the MCS connected to the bus i is prevented in time interval t. The power constraint during the charging operation of EVs by PCSs is given in (15). The rate limits in (12), (13) and (15) are determined considering the power values of charging sockets and EVs in commercial applications. The battery state-of-energy (SOE) is determined by Eq. (16) by adding or subtracting the changes in time interval t according to the charging, discharging or travel mode of the MCS. The SOE of the battery is decreased by the energy consumption depending on the route traveled and the consumption due to the service provided to the EVs, while it is increased by the charging operations at the time intervals and bus nodes decided by the algorithm. The lower and upper limit and initial SOE values of the MCS's battery are defined in (17) and (18), respectively.

Connection and routing constraints of MCS are given by (19) – (23). The connection of the MCS to a single bus in time interval t is provided by (19), while the detection of the travel status of MCS is determined by (20). The travel status variable is a binary variable used to identify the time periods when the MCS is in mobility between two bus nodes. Besides, the connection of the MCS to the destination bus is prevented by (21) before the required period for its travel between departure and arrival bus nodes is passed. Status detection of the MCS departing from a bus node and arriving at a bus node and preventing both arrival and departure of the bus i in time interval t are performed by (22) and (23), respectively.

$$\sum_{i} m1_{i,t} \leq 1 \; \forall t \tag{19}$$

$$m2_{t} = 1 - \sum_{i} m1_{i,t} \; \forall t \tag{20}$$

$$\sum_{t-T_{i,j}+1}^{t} m4_{i,t} \leq 1 - m3_{j,t} \; \forall t, i, j \tag{21}$$

$$m3_{j,t} - m4_{i,t} = m1_{i,t} - m1_{i,(t-1)} \; \forall i, t \tag{22}$$

$$m3_{j,t} + m4_{i,t} \leq 1 \; \forall i, t \tag{23}$$

Mathematical model equations that are taken from [28] are used to calculate the energy consumption of MCS. Total traction force $F_{v,tt}^{t}$ in (24) comprises four main forces that are aerodynamic drag force, $F_{v,tt}^{a}$, rolling friction force, F_{tt}^{r}, gravity force, F_{tt}^{g}, and acceleration force, $F_{v,tt}^{ac}$. Based on the total traction force and the speed of the MCS, the required mechanical power is calculated by Eq. (29). Besides, as seen in Eq. (30), the mechanical power is divided by the efficiency of the MCS and the required electrical power is determined, and the amount of energy required to travel between two bus nodes is calculated by (31). As a result, the objective function (1) is minimized according to the equations and constraints (2) – (31).

$$F_{v,tt}^{t} = F_{v,tt}^{ac} + F_{v,tt}^{a} + F_{tt}^{r} + F_{tt}^{g} \; \forall v, tt \tag{24}$$

$$F_{v,tt}^{a} = \frac{1}{2}.\rho.A.C_{d}.(V_{v,tt}^{MCS} - V_{v,tt}^{W})^{2} \; \forall v, tt \tag{25}$$

$$F_{tt}^{r} = M^{MCS}.g.C_{rr}.\cos(\theta) \; \forall tt \tag{26}$$

$$F_{tt}^{g} = M^{MCS}.g.\sin(\theta) \; \forall tt \tag{27}$$

$$F_{v,tt}^{ac} = f_{m}.M^{MCS}.\alpha \; \forall v, tt \tag{28}$$

$$P_{v,tt}^{vm} = F_{v,tt}^{t}.V_{v,tt}^{MCS} \; \forall tt \tag{29}$$

$$P_{v,tt}^{ve} = \frac{P_{v,tt}^{vm}}{\eta_{d}} \; \forall tt \tag{30}$$

$$EC^{MCS} = \sum_{tt} \left(P_{v,tt}^{ve}.\Delta T\right) \tag{31}$$

The equations and constraints of the electrical network and MCS models in the designed algorithm are expressed by (1) – (31). The schematic of the proposed optimization algorithm consisting of the main steps is presented in Fig 2.

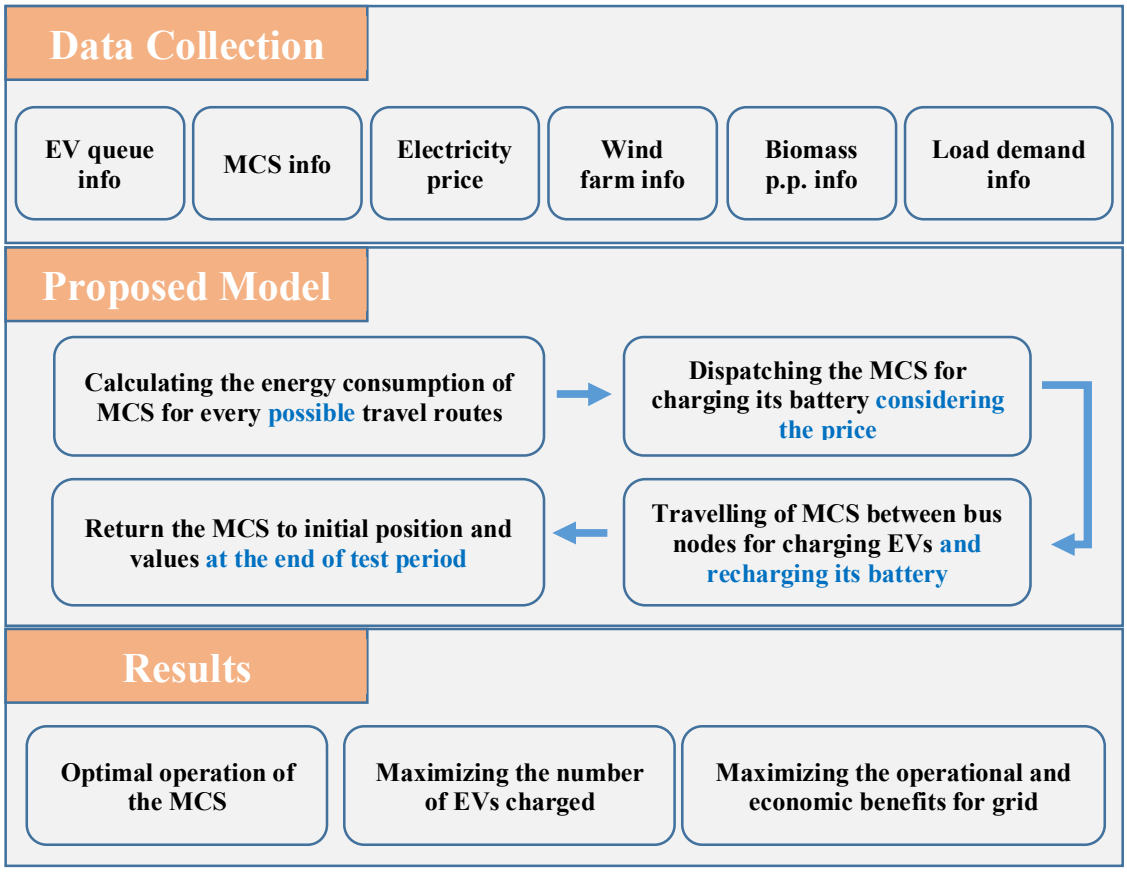

Fig. 2. Schematic representation of the proposed optimization algorithm.

3. Results and Discussion

3.1 Input Data

The considered 15-bus distribution system data are presented in Table 1 [29]. Line parameters are indicated as per unit. Base voltage, base apparent power and base impedance are selected as 12.66 kV, 100 kVA and 1602 Ω, respectively.

Any EV consumes energy according to its own and environmental parameters during its journey from a departure location to its destination. The energy consumption of the MCS during its travel between the bus nodes to charge its battery or to provide charging services to EVs is calculated according to the values in Table 2. In addition, the battery system energy density of the MCS is assumed to be approximately 265 kWh/kg [30]. While the EV manufacturers produce vehicles with different battery capacities and specific features, the batteries of the EVs are charged with different charging technologies. In this study, common charging technologies are examined, and it is assumed that EVs demanding three different charging powers, 7 kW, 11 kW and 22 kW, come to PCS points to receive charging service. Examples of EV types that demand these rated powers are Honda E (7kW), Audi E-Tron (11kW) and Renault ZOE (22kW) [31]. Besides, with minor changes to be made in the proposed algorithm, it can be applied if the EVs that demand more variety of rated charging power will be used.

The optimum operating location and time of the MCS vary according to the capacity and power characteristics of the MCS's battery. The SOE limits of the battery and energy flow parameters of MCS and PCS sockets are as given in Table 3. The MCS has a battery with a capacity of 2500 kWh and 18 charging sockets while the PCS has 10 charging sockets. Each socket owned by the MCS and PCS is an AC charging equipment with a nominal power of 22 kW. It is to be noted that the value of some parameters and variables of power grid and MCS model are multiplied by the base for accurate calculations as these units are defined as pu.

The load demand data of each bus node used in the study are obtained from the local distribution network operator, and the generated power data of the wind farm and biomass power plant (shown in Fig. 3) are obtained from the small-scale power plants belonging to an energy company in Turkey. While the MCS can charge its batteries from five different bus nodes, it only provides service at the PCS points due to the large space requirement for EVs during the charging service. The PCS points are located at Bus 4 and Bus 10, and the number of EVs arriving at PCSs to receive charging service is as seen in Fig. 4. In order to avoid the unnecessary and inefficient use of the MCS, the optimization algorithm considers the order of priority between the MCS and PCS. If the MCS is next to a PCS point, the PCS sockets are not used until all the MCS sockets are in use. Thus, the low-capacity use of the MCS is prevented and the operational contribution to the grid is provided at the maximum level since the energy stored in the battery will be used during the charging service.

The MCS's destination is determined by the EVs waiting for charging service and energy prices, as well as the travel time between departure and destination. The required time interval that belongs to the possible MCS routes to travel can be seen in Table 4. The algorithm ensures that the MCS battery does not fall below the minimum SOE value for the health of the battery during the test period, and that it has the initial SOE value at the end of the test period.

The proposed optimization algorithm is tested by using various operating modes of the MCS and two different electric market mechanisms as the extended work of [32] and the most optimum operating mode is aimed to be determined. The main objective of evaluating different cases is to provide the maximum service by the use of MCS to the EV users who prefer to receive the charging service in the PCS that has different peak hours. Besides, using an MCS can provide economic and operational advantages to PCS owners compared to the PCS expansion costs.

Table 1. Line parameters of the distribution system considered

Line	From	To	R [pu]	X [pu]	Line	From	To	R [pu]	X [pu]
L1	1	2	0	0	L8	7	9	0.11	0.11
L2	2	3	0.075	0.1	L9	8	10	0.11	0.11
L3	3	4	0.08	0.11	L10	8	11	0.08	0.11
L4	3	5	0.09	0.18	L11	2	12	0.11	0.11
L5	5	6	0.04	0.04	L12	12	13	0.09	0.12
L6	2	7	0.11	0.11	L13	12	14	0.08	0.11
L7	7	8	0.08	0.11	L14	14	15	0.04	0.04

Table 2. MCS and environmental parameters to calculate energy consumption

Parameter	Value	Parameter	Value
Coefficient of rolling resistance	0.02	Aerodynamic drag coefficient	0.5
Mass of MCS	14000 kg	Wind speed	0 m/s
Mass factor	1.05	Road slope angle	0 °
Air density	1.225 kg/m^3	Gravity of Earth	9.8 m/s^2
Vehicle frontal area	4 m^2	Efficiency of MCS	0.9

Table 3. MCS & PCS parameters for energy exchange

Parameter	MCS	PCS
CE^{MCS}	0.95	-
DE^{MCS}	0.95	-
$R^{MCS,ch/PCS,PD}$	22 kW/socket	22 kW/socket
$R^{MCS,dis}$	22 kW/socket	-
$SOE^{MCS,ini}$	200 kWh	-
$SOE^{MCS,min}$	200 kWh	-
$SOE^{MCS,max}$	2500 kWh	-

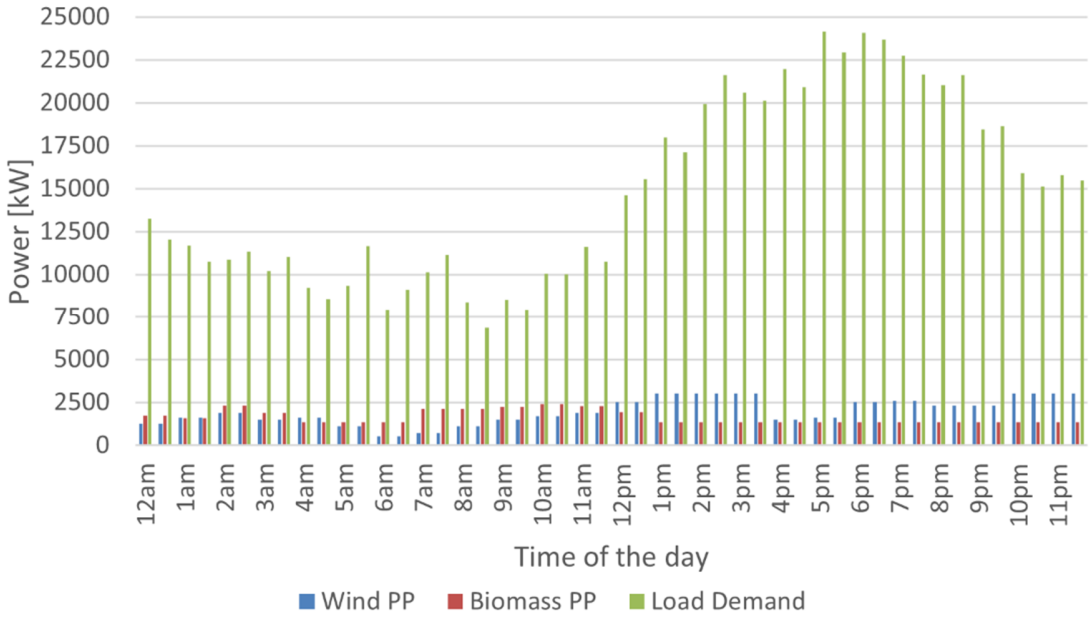

Fig. 3. Total load demand and power generation of RESs.

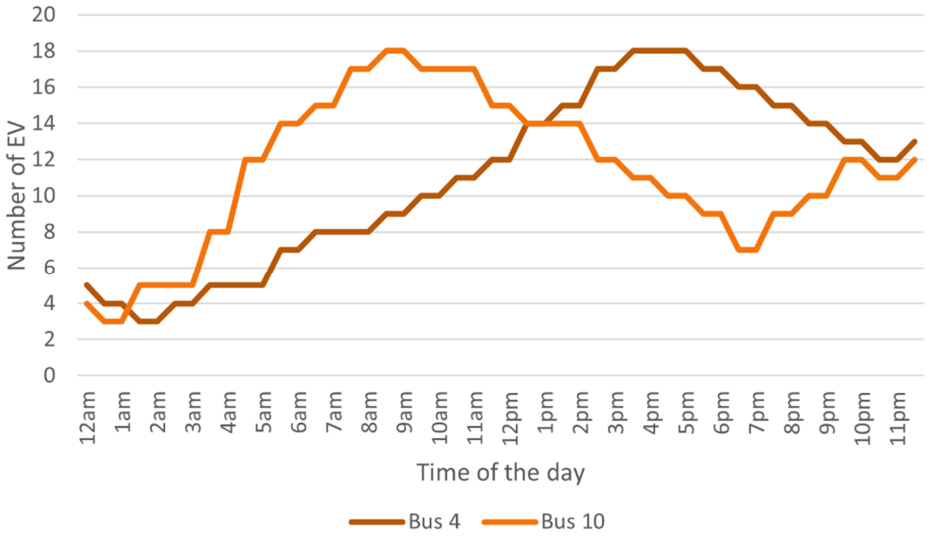

Fig. 4. The number of EVs requesting charging service at Bus 4 and Bus 10.

Table 4. Required time interval to travel between bus nodes

Road	From [Bus]	To [Bus]	Period [t]	Road	From [Bus]	To [Bus]	Period [t]
R1	B1	B4	3	R6	B4	B10	2
R2	B1	B6	1	R7	B4	B13	2
R3	B1	B10	3	R8	B6	B10	2
R4	B1	B13	2	R9	B6	B13	2
R5	B4	B6	3	R10	B10	B13	1

3.2 Simulation and Results

Five different cases are taken into consideration in order to evaluate the performance of the proposed model:

- **Case 1:** MCS is unavailable and energy tariff is fixed pricing.
- **Case 2:** MCS is movable and energy tariff is fixed pricing.
- **Case 3:** MCS is fixed at Bus 4 and energy tariff is fixed pricing.
- **Case 4:** MCS is movable and energy tariff is dynamic pricing level 1.
- **Case 5:** MCS is movable and energy tariff is dynamic pricing level 2.

A time granularity of 30 min (i.e., 0.5 h) is used in all five cases. The constrained optimization algorithm is evaluated on General Algebraic Modeling System (GAMS) version 25.1.3 by using MOSEK solver, which is frequently used in conic programming optimization. Besides, in this study, the mixed integer linear programming (MILP) method, whose efficiency was approved in the literature, is employed. The study is carried on a 2.21 GHz, quad-core i7-8750H processor PC with 16GB of RAM. MOSEK solver's

default values for the stopping criteria and the iteration limit are selected as 1.0e-6 and 1000000, respectively. In all cases, the proposed algorithm generates the optimum results before the specified termination values.

In Case 1, the service provided by the PCSs to EVs that come to receive charging service in a distribution network with fixed energy price is evaluated. The main purpose of examining Case 1 is to reveal the effectiveness of the MCS by comparing with the results of the other cases. The PCSs connected to Bus 4 and Bus 10 provide charging services to the maximum number of EVs by operating at full capacity. When more EVs arrive at the PCS points than the maximum number of sockets, there will be the missing vehicles or the EVs that cannot be charged, as shown in Fig. 5. Besides, it is clear that more charging sockets are needed on Bus 10 between 4:00 am and 4:00 pm and on Bus 4 between 10:00 am and 11:00 pm, as seen in Fig. 5. In Case 1, during the test period, the numbers of charged and missing EVs are 827 and 247, respectively, as seen in Fig. 6. In addition, PCSs can charge 77% of EVs in the queue within their capabilities, while 23% of the EVs in demand cannot be serviced.

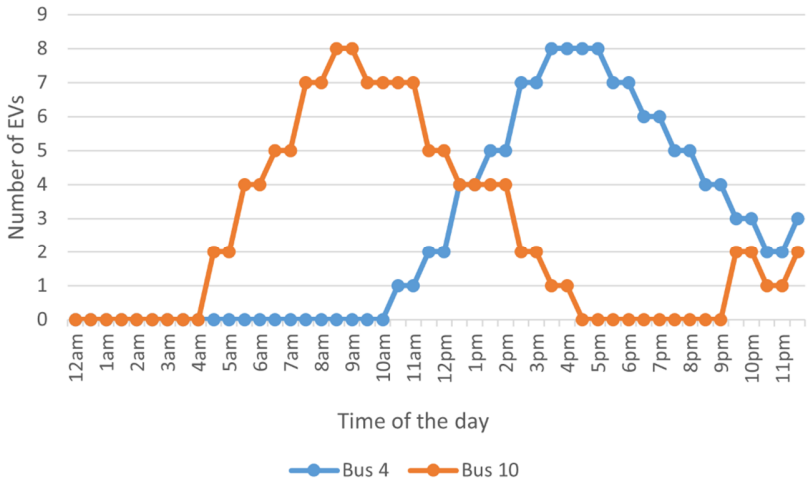

Fig. 5. Number of EVs not charged due to reaching the full capacity for Case 1.

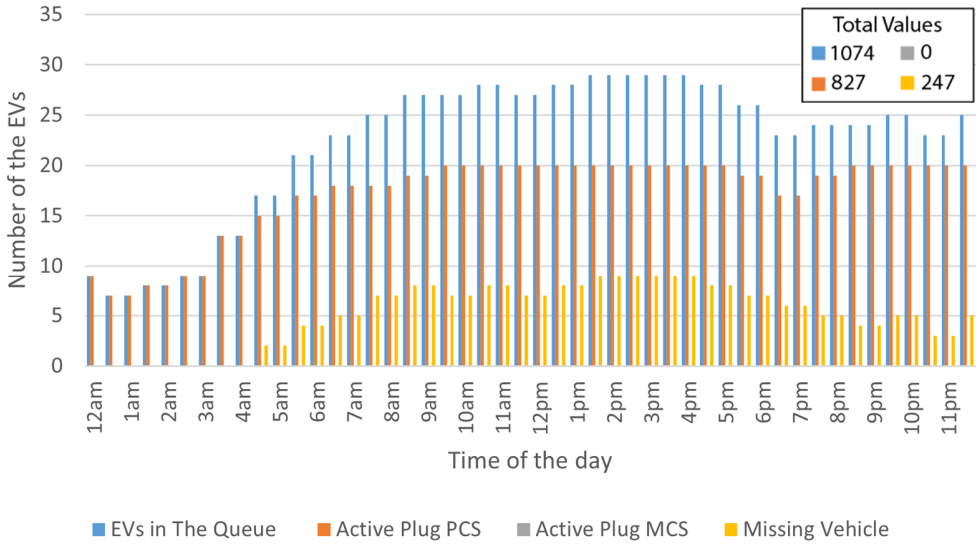

Fig. 6. Comparison of the PCS, MCS, EV queue and missing EV for Case 1.

It should be noted that new socket installation can be considered to reduce the missing EVs as the first option so that the PCS can charge more EVs. However, the electrical network infrastructure may not be sufficient or it may be costly to install extra sockets. In Case 2, in addition to Case 1, it is assumed that there is an MCS with a 2500 kWh battery and 18 charging sockets in the system. It is to be noted that in all cases where the MCS is involved, it is aimed to maximize the number of EVs charged by operating at PCS points that especially have different peak periods.

As shown in Fig. 7, the MCS provides the most optimum service by performing multiple charging and discharging operations at different time intervals. Moreover, it is observed that the SOE increases at different time intervals depending on the charging operations and reaches up to 2000 kWh. It is also seen that SOE decreases due to serving the EVs and has initial SOE value at the end of the test period. As mentioned before, the optimization algorithm determines the operation bus nodes of the MCS by taking into account the required travel period between the bus nodes. The four bus nodes and the connection time of the MCS during the test period can be seen in Fig. 8. With the inclusion of the MCS in the designed system, there is a considerable change in the number of the EVs served. The results obtained after the service given by the MCS according to the EV queue of Bus 4 and Bus 10 are given in Fig 9. During the test period, 567 and 419 EVs are charged by PCS and MCS, respectively as given in Fig. 10. Besides, the number of EVs that cannot be serviced is determined as 88 EVs, decreasing by 64.3% compared to Case 1. Furthermore, 39% of the EVs queuing at Bus 4 and Bus 10 are served by MCS at different time intervals, reducing the percentage of unserved vehicles to 8%.

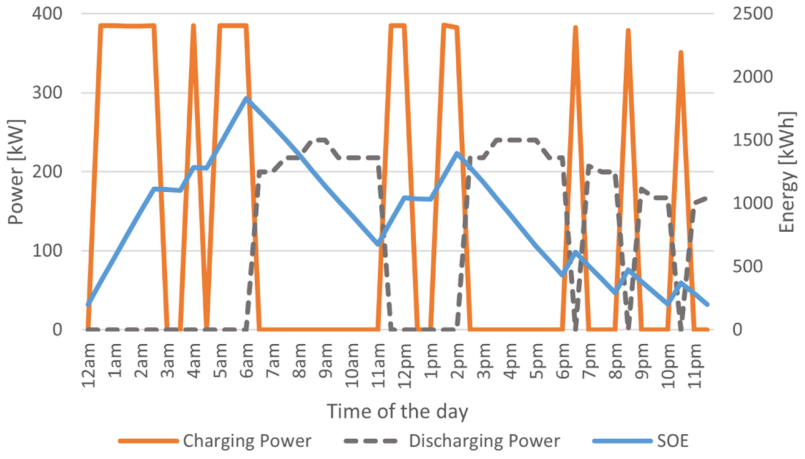

Fig. 7. Power exchange and SOE of MCS's battery for Case 2.

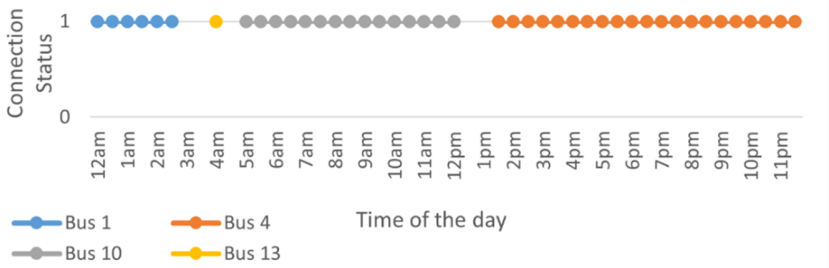

Fig. 8. MCS connection status during the test period for Case 2.

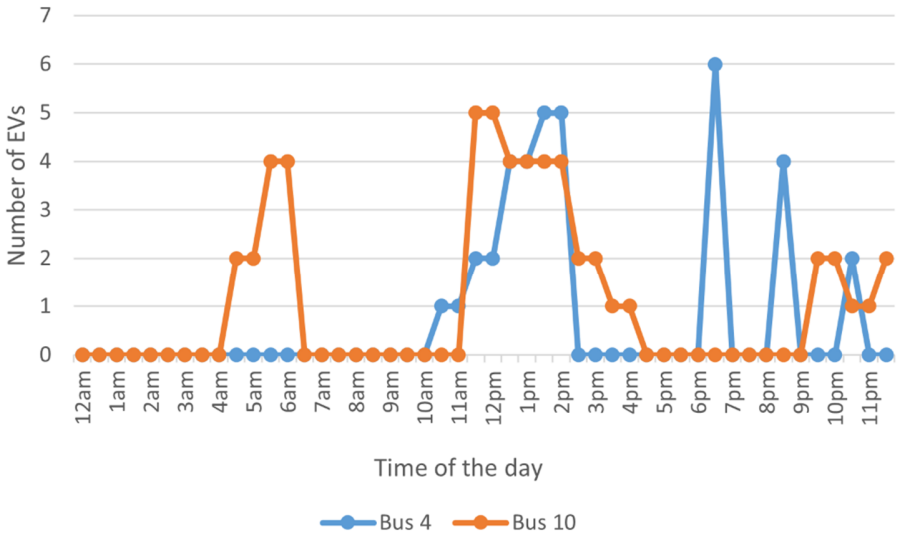

Fig. 9. Number of EVs not charged due to reaching the full capacity for Case 2.

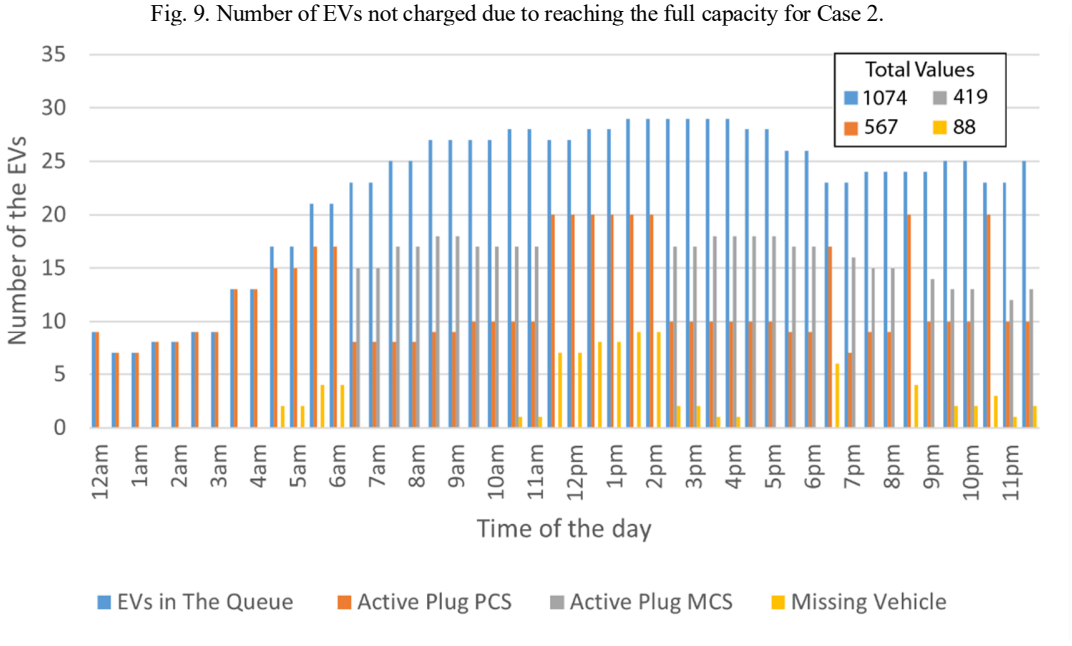

Fig. 10. Comparison of the PCS, MCS, EV queue and missing EV for Case 2.

As mentioned previously, the PCS expansion may be an option to serve more EVs. In Case 3, the fixed operation of the MCS at one of the two PCS points is evaluated in order to reveal the results to be obtained with the expansion. Besides, it can be considered that the PCS has an ESS thanks to the battery of MCS. As the PCS on Bus 4 is sufficient for the EV charging demand up to 10:00 am, the MCS battery reaches its full capacity during the same time period. Due to the increase in the number of EVs arriving after 10:00 am, it is seen in Fig. 11 that the MCS provides the charging service to the EVs. In this operating mode, since the MCS is used as fixed, the connection point during the test period is Bus 4 as seen in Fig. 12.

The constrained optimization algorithm calculates the optimum value of the objective function by determining the charging-discharging operations of the MCS. As shown in Fig. 13, almost all of the EVs that come to Bus 4 for the charging service are charged. It is therefore concluded that the results of the operation at Bus 4 with the help of MCS are effective and the expansion is

reasonable. However, the EVs greater than the maximum number of sockets are rejected as the MCS cannot serve on Bus 10. When mobile and fixed operations are compared, the number of the missed EVs increases from 88 to 126 with an increase of 43.18% in the fixed operation. As seen from the outputs of the PCS, MCS, EV queue and missing EV in Fig 14, PCS and MCS serve 572 and 376 EVs, respectively. During fixed operation at Bus 4, 53% of the total EVs are served by PCSs and 35% by MCSs.

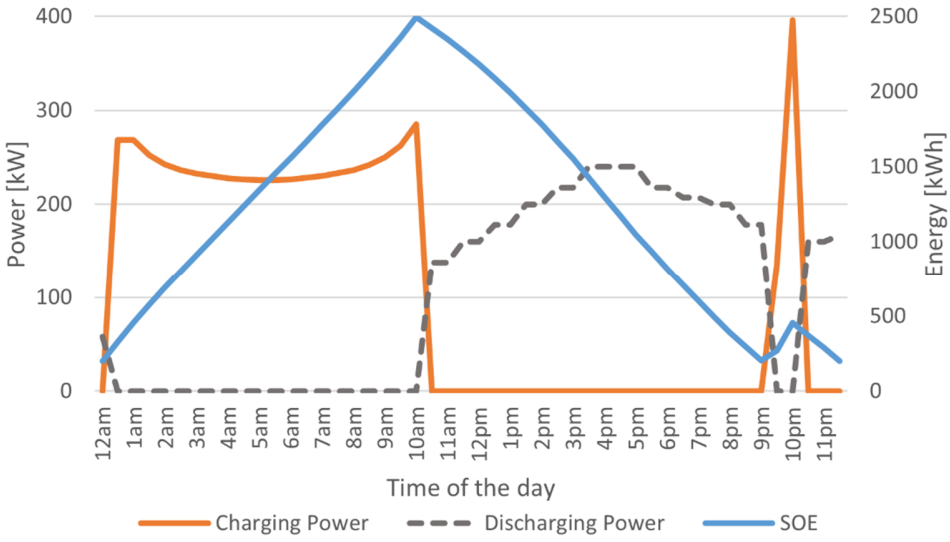

Fig. 11. Power exchange and SOE of MCS's battery for Case 3.

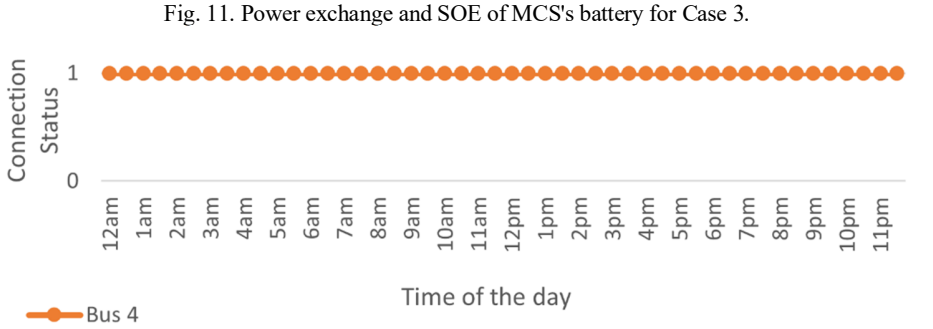

Fig. 12. MCS connection status during the test period for Case 3.

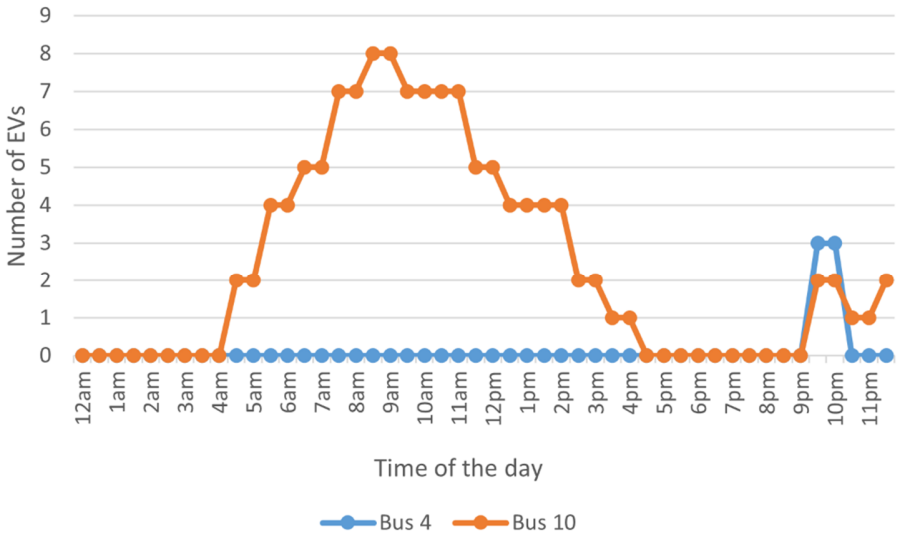

Fig. 13. Number of EVs not charged due to reaching full capacity for Case 3.

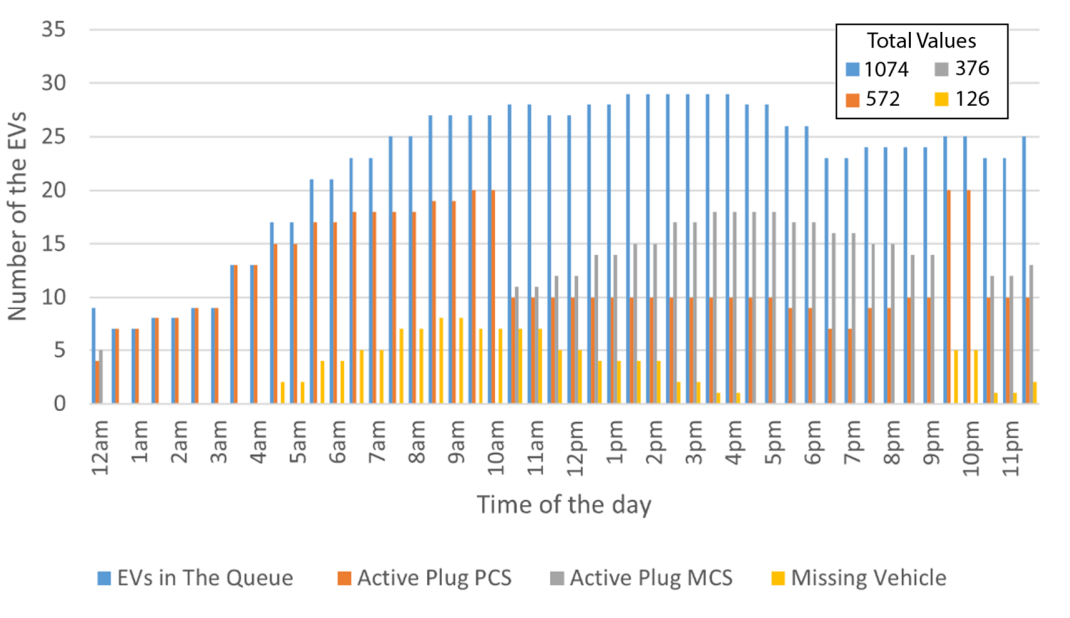

Fig. 14. Comparison of the PCS, MCS, EV queue and missing EV for Case 3.

Case 3 presents the results when the MCS is fixed at Bus 4. It is to be noted that the case of the MCS fixed at Bus 10 is tested in the study, however, the relevant figures are not given for the sake of the brevity. The optimum operation of the MCS will be different for this case due to the number of EVs arriving at the PCSs for charging service and the fact that their arrival time are different from each other. While the number of PCS and MCS sockets remains the same, the change in the charging power demand of the EVs causes great changes in the number of the EVs that cannot be served. MCS serves 354 EVs when connected to Bus 10, and the number of EVs that cannot be serviced due to insufficient sockets is 147. The comparison results of Bus 4 and Bus 10 clearly show that the characteristics such as EV density and busy period of each PCS should be examined for an expansion decision.

Assessing the efficiency of the designed distribution system in different electricity markets may provide further insight into its economic and operational benefits. The hourly electricity prices are assumed to be variable in Case 4 during the test period as shown in Fig. 15. Thus, in this case, when the MCS provides maximum service to EVs, the charging-discharging time of the MCS battery is decided depending on the electric market. For this purpose, electricity prices are also included in the objective function and changed as seen in Eq. (32).

$$Minimize\ MV = \sum_t \sum_i ((P_{i,t}^{CPD} - P_{i,t}^{MCS,dis} - P_{i,t}^{PCS,PD}) \cdot \Delta T \cdot Price_{i,t}) + \sum_t \sum_i ((P_{i,t}^{MCS,ch} - P_{i,t}^{MCS,dis}) \cdot \Delta T \cdot Price_{i,t}) \quad (32)$$

As an additional advantage, economic benefits are achieved in Case 4 by charging the mobile battery of the MCS when electricity prices are lower and discharging when electricity is more expensive. Since both economic operation and the maximum EV service are aimed, it can be seen in Fig. 16 that the charging - discharging operations of the MCS battery are carried out by taking the hourly electricity price into account. Besides, MCS serves in four different bus nodes in total as shown in Fig. 17. As seen in Fig. 18, since the MCS provides more services on Bus 4, the number of missed EV on Bus 10 is higher. When Case 4 and

Case 2 are compared, it is seen that the number of EVs served by MCS has decreased by 28 in Case 4. However, Fig. 19 shows an increase of 10 EVs in the number of EVs served by PCS. It is obvious that the decrease in the number of EVs served by the MCS is occurred in order to achieve multiple economical and operational goals. As a result, in Case 4, taking energy prices into account, 54% of the service takes place at PCS and 36% at MCS, with a small increase in the number of EVs served compared to Case 3.

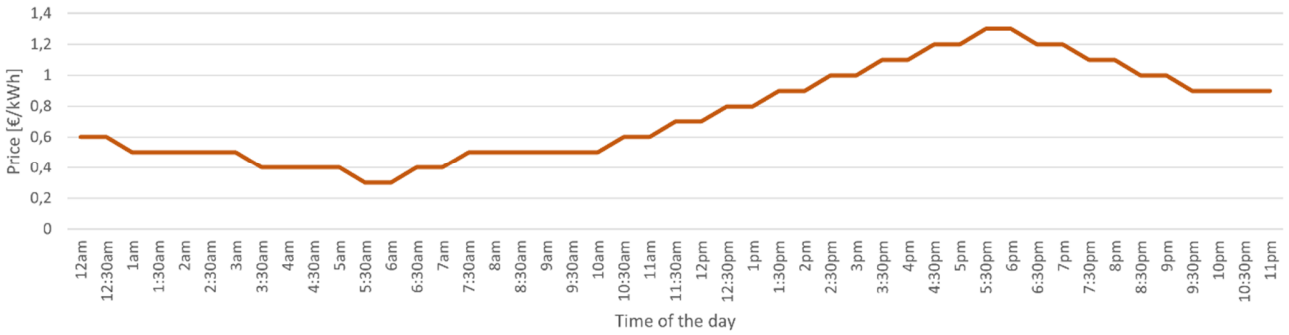

Fig. 15. Electricity price change during the test period for Case 4.

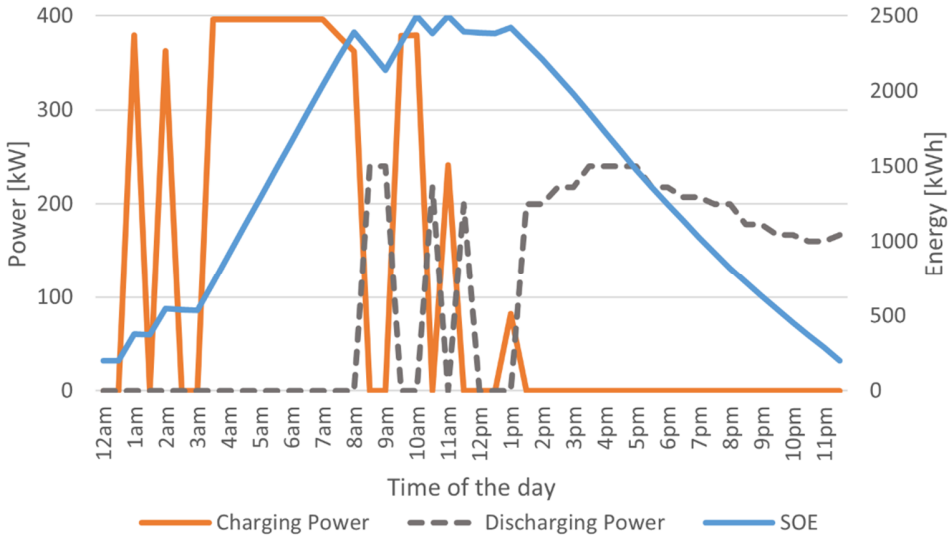

Fig. 16. Power exchange and SOE of MCS's battery for Case 4.

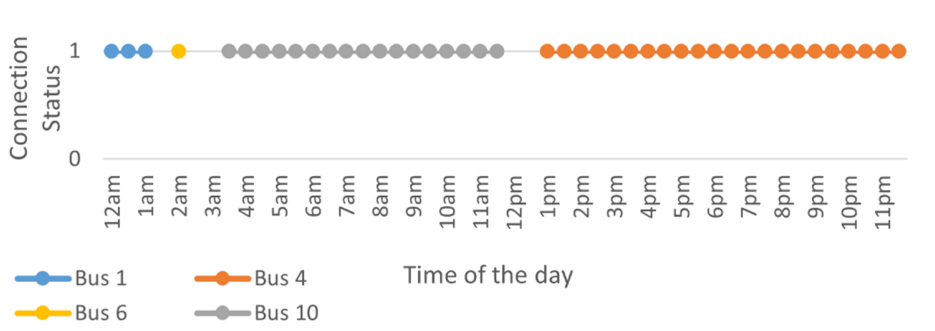

Fig. 17. MCS connection status during the test period for Case 4.

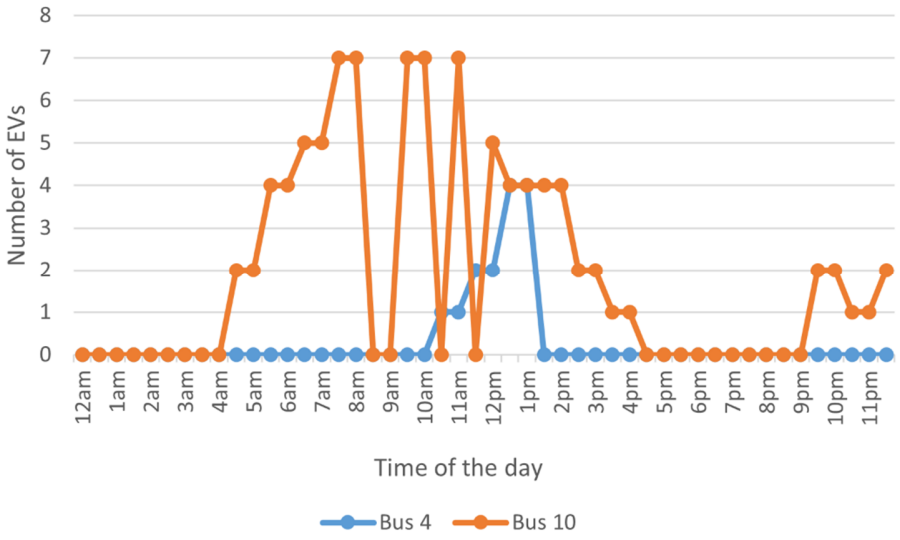

Fig. 18. Number of EVs not charged due to reaching the full capacity for Case 4.

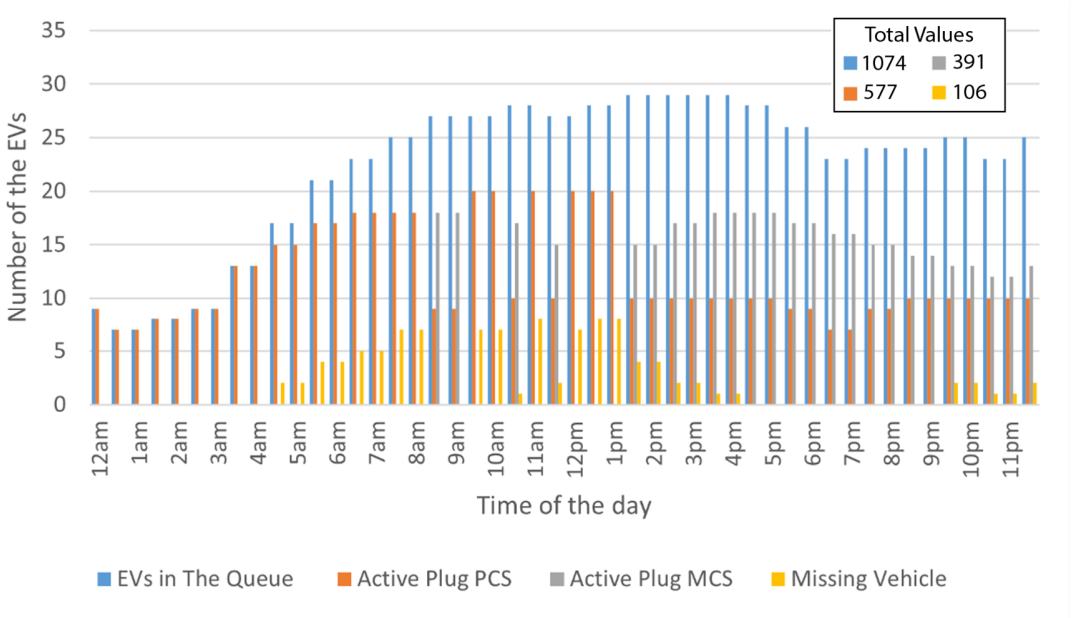

Fig. 19. Comparison of the PCS, MCS, EV queue and missing EV for Case 4.

Various incentives are provided in most of the countries to increase the share of energy produced by RESs in the energy mix, which generally results in reduced energy costs. Based on this idea, in Case 5, it is assumed that cheaper energy can be accessed especially during off-peak periods in the bus nodes where the wind farm and biomass power plant are located. The variation of the energy prices of the five bus nodes where the MCS can charge its battery is shown in Fig. 20. First, it can be seen that the battery of the MCS is fully charged at Bus 6 until 7:00 am. When the charging bus node and time interval of the MCS are analyzed, it is seen that Bus 6 is chosen due to the price incentives of the wind farm and the time interval is the period when prices are low. Similar to Case 4, the MCS provides charging service to EVs mostly on Bus 4 after 1:00 pm and completes the test period with the initial SOE value. The charging-discharging operations of the MCS and the change of SOE are shown in Fig. 21. As can be seen from

Fig. 22, the MCS visits the bus nodes by taking the price advantage of RESs. The graph of the number of the missed EV is given in Fig. 23 for the optimum use of the MCS and PCSs sockets in Case 5. During the test period, the MCS and PCSs charge 390 and 577 EVs, respectively, as given in Fig. 24. The number of missed EVs in Case 4 is 106 while it is 107 in Case 5. When Fig. 19 and Fig. 24 are analyzed, the values in Case 4 and Case 5 are fairly similar. Accordingly, the percentage of the EVs served by PCS and MCS is calculated as almost the same value in Case 4 and Case 5. However, when the economic benefit of dynamic pricing in Case 4 and Case 5 is examined by considering the benefit to be obtained by charging the battery of the MCS in the low energy price period and by providing the charging service in the expensive price period, it is determined as 1236.84 € and 1812.73 € for Case 4 and Case 5, respectively. The results prove that the economic benefits can be increased without losing the operational benefit in markets with the incentive mechanisms.

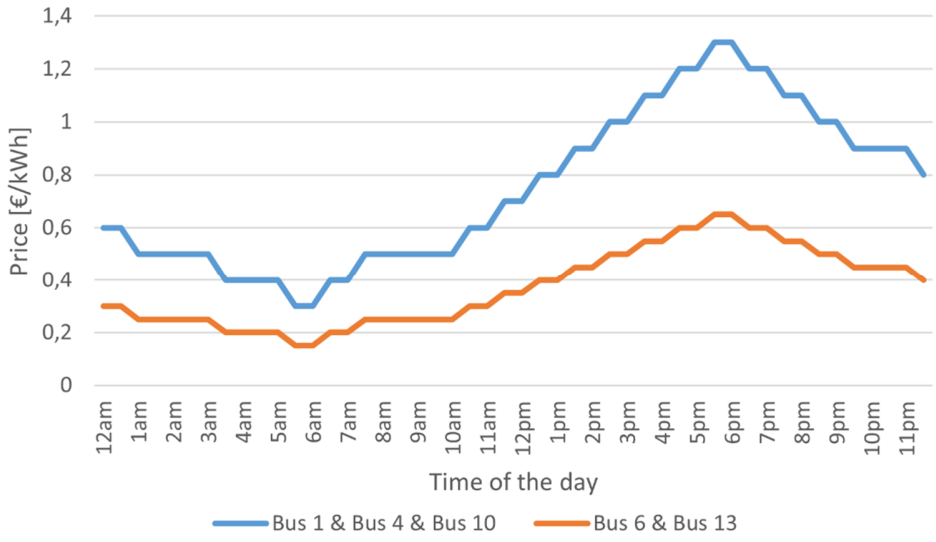

Fig. 20. Electricity price change during the test period for Case 5.

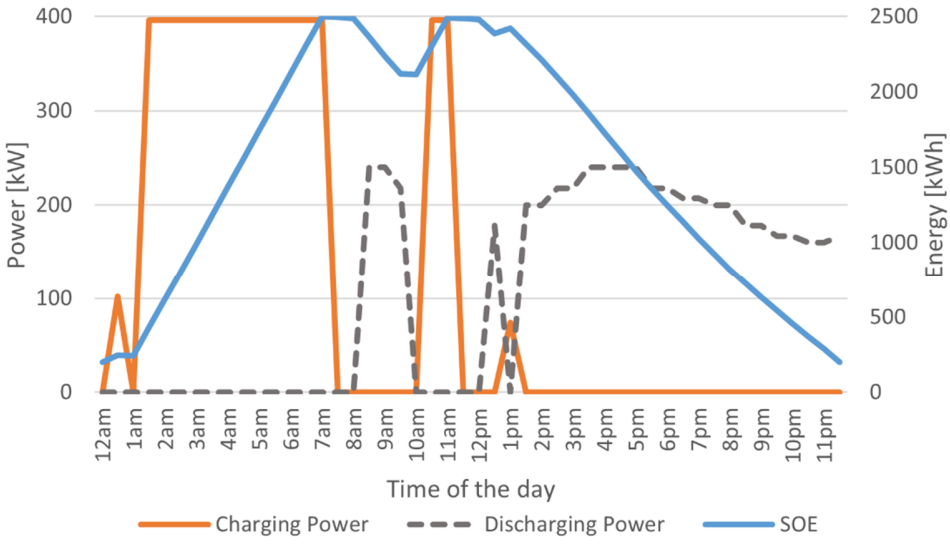

Fig. 21. Power exchange and SOE of MCS's battery for Case 5.

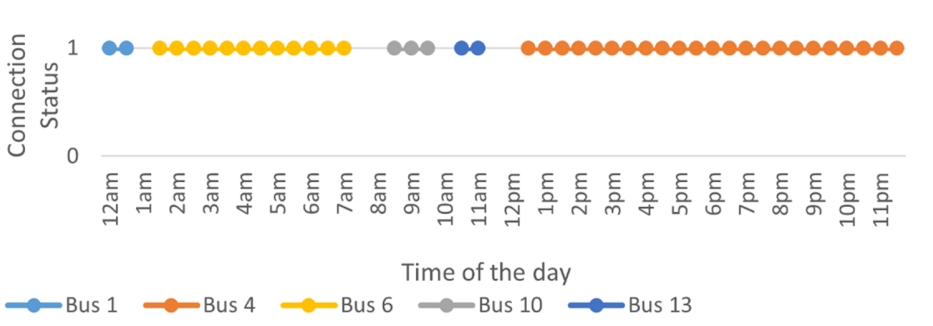

Fig. 22. MCS connection status during the test period for Case 5.

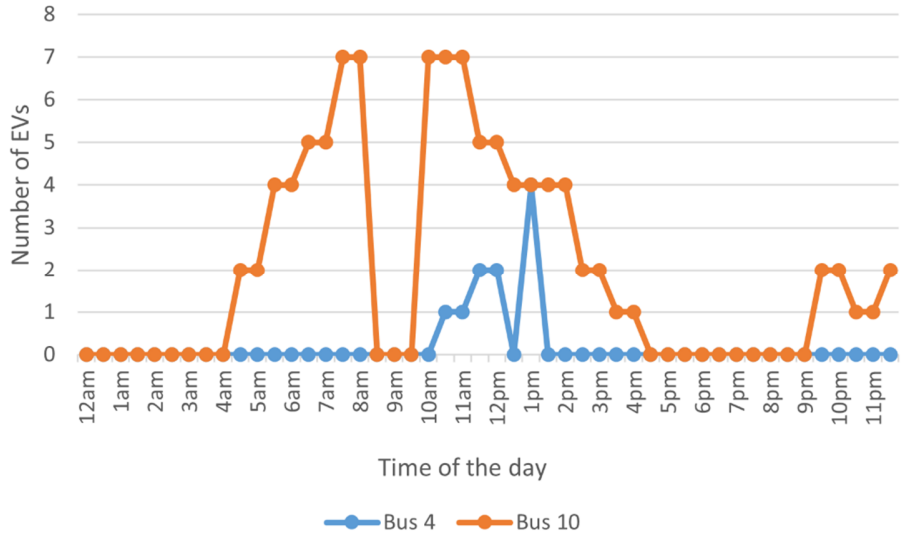

Fig. 23. Number of EVs not charged due to reaching the full capacity for Case 5.

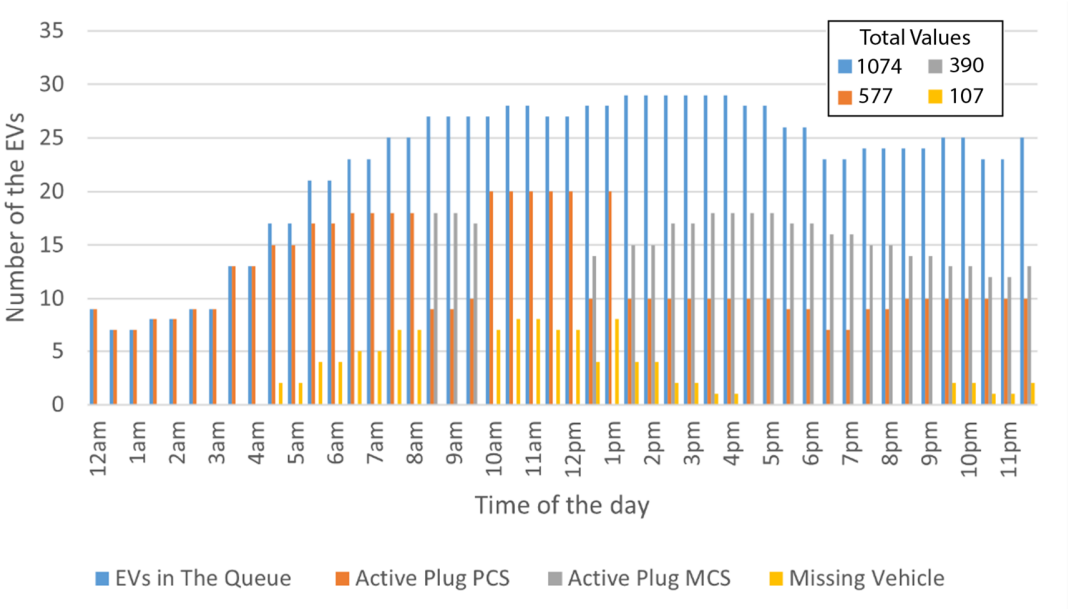

Fig. 24. Comparison of the PCS, MCS, EV queue and missing EV for Case 5.

4. Discussion

The use of EVs and MCS applications is accelerated by the technical, legal and social contribution of all stakeholders. Particularly, the MCS applications will be needed more in the near future as EVs become widespread and the developments in battery technologies will reduce the size and weight of the MCSs to be used. Besides, MCS might remove one of the barriers to higher EV use by offering a fast and economical solution in areas where the electricity grid infrastructure is insufficient.

Another important issue is that electrical energy demand and energy prices are directly proportional. In order to operate more economically, the MCS's battery stores the energy in the low demand period, and it uses the energy in the battery when it is expensive in peak energy period. Thus, it contributes to flatten the load curve by making the valley filling and peak shaving operations in the network, while making a positive impact on the reliability and sustainability of the system.

Moreover, the grid-free emergency mobile EV charging stations can be seen in real applications in parallel with the increasing amount of EVs. MCS systems, which provide service in AC and DC mode at different power levels, are used without the need for infrastructure and large installation areas. As MCS can be designed with the desired battery capacity and features, it is likely to be preferred by enterprises such as service stations, car dealerships and EV fleet managers to increase the customer satisfaction.

5. Conclusions

The expansion of the PCSs and hence the relevant unnecessary investments can be avoided with the use of MCSs. The constrained optimization algorithm proposed in this study determines the time and place to use an MCS for serving the highest possible EVs in all cases. The results prove that the use of the MCS brings about economic and operational benefits to the charging station owners and the distribution system operator.

An operational improvement of 64.3% in Case 2 that serves the most EVs is achieved when compared to Case 1 that does not include the MCS. The results of Case 3 examining the enlargement made in the PCSs with high charging demand show that the use of the MCS is more advantageous due to the operation flexibility. Besides, when Case 3 results are evaluated, they show that the idea of the stationary ESS usage without the charging sockets in the fixed charging stations can provide limited operational and economic benefits. Dynamic energy prices in Case 4 and Case 5 have an impact on MCS's service points and time interval decision to ensure economic benefits. In particular, this situation leads to an increase of approximately 20% in the number of EVs that cannot charged. Therefore, the total energy taken from the system is used during the test period. From an economic point of view, there is no profit since the energy prices are fixed in Case 2 and Case 3 and the net energy change is zero in the MCS battery. Moreover, in Case 5, where the incentive is included, approximately 46% more profit is made compared to Case 4.

The number of MCS in the system, the battery capacity of the MCS and the number of sockets are all effective on the results. While more sockets increase the number of EVs served, the larger capacity battery has both economic and operational advantages.

Therefore, the structure of the region where the MCS will be used should be taken into account in determining the MCS properties. It is to be noted that the technology mentioned in the study can be used to ensure system reliability during the reinforcement of the grid infrastructure as a result of increasing energy demand for better integration of RESs, and to provide more flexible and economical operation instead of the ESSs currently in place. As a future study, the efficiency of the proposed algorithm can be tested by using different numbers of MCSs with various capacity and sockets on different bus systems such as IEEE 33. In addition, the initial purchase, maintenance, and operating costs of MCS can be taken into account for a detailed economic analysis.

Acknowledgement

This work of A. Taşcıkaraoğlu is supported by the Turkish Academy of Sciences (TUBA) within the framework of the Distinguished Young Scientist Award Program (GEBIP).

REFERENCES

[1] IEA, "World Energy Outlook 2021," IEA Publ., p. 15, 2021.
[2] EIA, "International Energy Outlook 2021," U. S. Department of Energy, pp. 1–40, 2021.
[3] EIA, "Annual Energy Outlook," U.S. Energy Inf. Adm., 2022.
[4] International Energy Agency (IEA), "Global EV Outlook 2022 - Securing supplies for an electric future," Glob. EV Outlook 2022, p. 221, 2022.
[5] S. Alotaibi, S. Omer, and Y. Su, "Identification of Potential Barriers to Electric Vehicle Adoption in Oil-Producing Nations—The Case of Saudi Arabia," Electricity, vol. 3, no. 3, pp. 365–395, 2022.
[6] K. Yadav and A. Sircar, "A review on electric vehicle transport policy of India with certain recommendations," MRS Energy Sustain., doi:10.1557/s43581-022-00048-6, pp. 1–11, 2022.
[7] Y. R. Yin, Y. Li, and Y. Zhang, "Influencing factor analysis of household electric vehicle purchase intention of HaiNan Free Trade Port under the background of low-carbon lifestyle," Energy Reports, vol. 8, pp. 569–579, 2022.
[8] E. Azadfar, V. Sreeram, and D. Harries, "The investigation of the major factors influencing plug-in electric vehicle driving patterns and charging behaviour," Renew. Sustain. Energy Rev., vol. 42, pp. 1065–1076, 2015.
[9] P. Richardson, D. Flynn, and A. Keane, "Optimal charging of electric vehicles in low-voltage distribution systems," IEEE Trans. Power Syst., vol. 27, no. 1, pp. 268–279, 2012.
[10] Z. Huang, Z. Guo, P. Ma, M. Wang, Y. Long, and M. Zhang, "Economic-environmental scheduling of microgrid considering V2G-enabled electric vehicles integration," Sustain. Energy, Grids Networks, vol. 32, p. 100872, 2022.
[11] F. R. Albogamy et al., "Real-Time Scheduling for Optimal Energy Optimization in Smart Grid Integrated with Renewable Energy Sources," IEEE Access, vol. 10, pp. 35498–35520, 2022.
[12] A. Moradipari and M. Alizadeh, "Pricing and Routing Mechanisms for Differentiated Services in an Electric Vehicle Public Charging Station Network," IEEE Trans. Smart Grid, vol. 11, no. 2, pp. 1489–1499, 2020.
[13] C. Li, L. Zhang, Z. Ou, Q. Wang, D. Zhou, and J. Ma, "Robust model of electric vehicle charging station location considering renewable energy and storage equipment," Energy, vol. 238, p. 121713, 2022.
[14] J. A. Domínguez-Navarro, R. Dufo-López, J. M. Yusta-Loyo, J. S. Artal-Sevil, and J. L. Bernal-Agustín, "Design of an electric vehicle fast-charging station with integration of renewable energy and storage systems," Int. J. Electr. Power Energy Syst., vol. 105, no. July 2018, pp. 46–58, 2019.
[15] A. T. Lemeski, R. Ebrahimi, and A. Zakariazadeh, "Optimal decentralized coordinated operation of electric vehicle aggregators enabling vehicle to grid option using distributed algorithm," J. Energy Storage, vol. 54, no. June, p. 105213, 2022.
[16] M. W. Khan and J. Wang, "Multi-agents based optimal energy scheduling technique for electric vehicles aggregator in microgrids," Int. J. Electr. Power Energy Syst., vol. 134, no. May 2021, p. 107346, 2022.
[17] P. Harsh and D. Das, "Optimal coordination strategy of demand response and electric vehicle aggregators for the energy management of reconfigured grid-connected microgrid," Renew. Sustain. Energy Rev., vol. 160, no. November 2021, p. 112251, 2022.

[18] M. A. Beyazıt, A. Taşcıkaraoğlu, and J. P. S. Catalão, “Cost optimization of a microgrid considering vehicle-to-grid technology and demand response,” Sustain. Energy, Grids Networks, vol. 32, p. 100924, 2022.

[19] A. K. Aktar, A. Taşcıkaraoğlu, S. S. Gürleyük, and J. P. S. Catalão, “A framework for dispatching of an electric vehicle fleet using vehicle-to-grid technology,” Sustain. Energy, Grids Networks, vol. 33, p. 100991, 2023.

[20] S. Afshar, Z. K. Pecenak, M. Barati, and V. Disfani, “Mobile charging stations for EV charging management in urban areas: A case study in Chattanooga,” Appl. Energy, vol. 325, no. April, p. 119901, 2022.

[21] M. Nazari-Heris, A. Loni, S. Asadi, and B. Mohammadi-ivatloo, “Toward social equity access and mobile charging stations for electric vehicles: A case study in Los Angeles,” Appl. Energy, vol. 311, no. January, p. 118704, 2022.

[22] M. U. Mutarraf, Y. Guan, L. Xu, C. L. Su, J. C. Vasquez, and J. M. Guerrero, “Electric cars, ships, and their charging infrastructure – A comprehensive review,” Sustain. Energy Technol. Assessments, vol. 52, no. PB, p. 102177, 2022.

[23] High-power charging trucks become mobile power sources. Available Online: https://newsroom.porsche.com/en/2020/company/porsche-high-power-charging-trucks-mobile-power-sources-22285.html (accessed on 24 October 2022)

[24] L. Liu, X. Qi, Z. Xi, J. Wu, and J. Xu, “Charging-Expense Minimization Through Assignment Rescheduling of Movable Charging Stations in Electric Vehicle Networks,” IEEE Trans. Intell. Transp. Syst., pp. 1–12, 2022.

[25] H. Saboori and S. Jadid, “Mobile battery-integrated charging station for reducing electric vehicles charging queue and cost via renewable energy curtailment recovery”. Int. J. of Energy Research, vol. 46, pp. 1077-1093, 2021.

[26] I. El-fedany, D. Kiouach, and R. Alaoui, “A Smart Coordination System Integrates MCS to Minimize EV Trip Duration and Manage the EV Charging, Mainly at Peak Times,” Int. J. Intell. Transp. Syst. Res., vol. 19, no. 3, pp. 496–509, 2021.

[27] M. Baradar and M. R. Hesamzadeh, “AC power flow representation in conic format,” IEEE Trans. Power Syst., vol. 30, no. 1, pp. 546–547, 2015.

[28] I. Şengör, A. K. Erenoğlu, O. Erdinç, A. Taşcikaraoğlu, and J. P. S. Catalão, “Day-ahead charging operation of electric vehicles with on-site renewabale energy resources in a mixed integer linear programming framework,” IET Smart Grid, vol. 3, no. 3, pp. 367–375, 2020.

[29] A. K. Erenoğlu and O. Erdinç, “Post-Event restoration strategy for coupled distribution-transportation system utilizing spatiotemporal flexibility of mobile emergency generator and mobile energy storage system,” Electr. Power Syst. Res., vol. 199, no. March, 2021.

[30] Battery System Energy Density Specifications Available Online: https://www.catl.com/en/solution/passengerEV/ (accessed on 24 October 2022)

[31] Electric Vehicle Specifications Available Online: https://ev-database.org/ (accessed on 24 October 2022)

[32] A. K. Aktar, A. Taşcıkaraoğlu and J. P. S. Catalão, "Optimal Charging and Discharging Operation of Mobile Charging Stations," 2022 International Conference on Smart Energy Systems and Technologies (SEST), 2022, pp. 1-6, doi: 10.1109/SEST53650.2022.9898463.